ACS OMEGA

http://pubs.acs.org/journal/acsodf

Article

Impact of a Novel Phosphoramide Flame Retardant on the Fire Behavior and Transparency of Thermoplastic Polyurethane Elastomers

Mengqi Li, Yajun Chen,* Zimeng Kong, Zhe Sun, and Lijun Qian

Cite This: *ACS Omega* 2023, 8, 18151−18164

Read Online

ACCESS | Metrics & More | Article Recommendations

ABSTRACT: In many application fields of thermoplastic polyurethane (TPU), excellent flame retardancy and transparency are required. However, higher flame retardancy is often at the expense of transparency. It is difficult to achieve high flame retardancy while maintaining the transparency of TPU. In this work, a kind of TPU composite with good flame retardancy and light transmittance was obtained by adding a new synthetic flame retardant named DCPCD, which was synthesized by the reaction of diethylenetriamine and diphenyl phosphorochloridate. Experimental results showed that 6.0 wt % DCPCD endowed TPU with a limiting oxygen index value of 27.3%, passing the UL 94 V-0 rating in the vertical burning test. The cone calorimeter test results showed that the peak heat release rate (PHRR) of the TPU composite was dramatically reduced from 1292 kW/m^2 (pure TPU) to 514 kW/m^2 by adding only 1 wt % DCPCD. With the increase of DCPCD contents, the PHRR and total heat release gradually decreased, and the char residue gradually increased. More importantly, the addition of DCPCD has little effect on the transparency and haze of TPU composites. In addition, scanning electron microscopy, Raman spectroscopy, and X-ray photoelectron spectroscopy were carried out to investigate the morphology and composition of the char residue for TPU/DCPCD composites and explore the flame retardant mechanism of DCPCD in TPU.

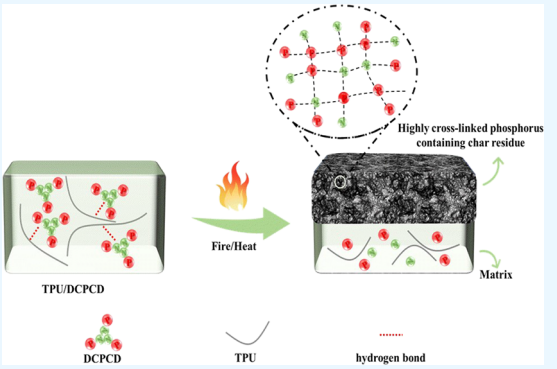

1. INTRODUCTION

Thermoplastic polyurethane (TPU) elastomer is a block polymer composed of soft and hard segments with excellent strength, impact resistance, and abrasion resistance. The soft segment is mainly composed of polyether or polyester and other oligomeric diols, accounting for 50−80% of the mass fraction of polyurethane. The hard segment is mainly composed of diisocyanate and chain extender, which mainly affects the high-temperature performance of the material.[1−4] The main application fields of TPU include pipes, synthetic leather, wires and cables, automobile fields, etc.[5−15] However, TPU is a flammable material, and its limiting oxygen index (LOI) is only about 20%. In addition, TPU emits a large number of toxic gases such as hydrocyanic acid and carbon monoxide during combustion and has a severe molten dripping phenomenon, which may further ignite other materials and cause rapid flame spread. Therefore, it will seriously endanger the safety of people's lives and property.[16−20] It is necessary to improve the flame retardancy of TPU.

There are two main types of flame retardant methods currently applied to TPU. The first is the preparation of inherently flame-retarded TPU, which is difficult to industrialize.[21−25] The second is the additive type, which is mainly used in the research and application field of flame retardant TPU.[26−32]

There are three types of additive flame retardants commonly used in TPU. First, inorganic traditional added flame retardants, such as aluminum hypophosphite, ammonium polyphosphate (APP), aluminum diethylphosphinate, melamine cyanurate and its derivatives, melamine polyphosphate, metal hydroxide, and expandable graphite.[33−50] However, these flame retardants generally have many problems, such as large addition amounts, low flame retardant efficiency, and influence on the mechanical properties of materials. Second, the new modified nano-additive flame retardants, such as MXene, Si_3N_4 nanosheets, COF, MOF, black phosphorus, graphene, boron nitride nanosheets, montmorillonite nanosheets, and carbon nanotubes.[18,51−59] Compared with inorganic conventional additive flame retardants, modified nano-additive flame retardants with a small additional

Received: March 4, 2023
Accepted: April 25, 2023
Published: May 10, 2023

Scheme 1. Synthesis of DCPCD

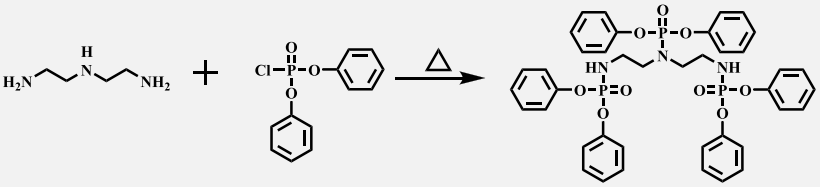

amount are found to have a lower peak heat release rate (PHRR) and better smoke suppression in cone calorimetric tests with low impact on the mechanical properties of TPU composites. However, it is difficult to obtain a high LOI value and high UL 94 level by adding a nano flame retardant in TPU, which cannot meet the demand for industrial products. In addition, the high cost and price also make it difficult to industrialize. In recent years, researchers have successively developed a variety of organic flame retardants and achieved good flame retardancy in TPU, most of which were prepared by organic synthesis methods based on phosphorus and nitrogen compounds.[60−66] Chen et al.[60,61] designed a novel piperazine-containing additive with phosphorus and alkynyl named poly(2-butyne-1,4-diol piperazine bisphosphonate) (PPBPP) to fabricate high-performance flame-retarding TPU. It was found that the introduction of piperazine groups into PPBPP achieved flame retardation and high performance of TPU simultaneously via induced crystallization. They also synthesized another flame retardant poly(2-butyne-1,4-diol phenylphosphonate) (PPBP) containing alkynyl groups to fabricate flame-retarded TPU. PPBP played a crucial role in enhancing the char-forming ability of TPU. Yang et al.[62] synthesized a Schiff-base polyphosphate ester (SPE) flame retardant as a novel flame retardant for TPU. Zhang et al.[63] prepared a novel flame retardant (ACS) by cross-linking chitosan with bis-(4-formylphenyl)-phenyl-phosphonate (ABPO). When 10 wt % APP/ACS (APP/ACS = 1:1) was incorporated into TPU, the LOI value of the TPU/APP/ACS sample reached 28.6% and passed the UL 94 V-2 rating. Liu et al.[64] synthesized a monocomponent intumescent flame retardant dimelamine pyrophosphate (DMPY) and incorporated it into the TPU matrix. When 15 wt % DMPY was incorporated, the samples of TPU/DMPY fulfilled UL 94 V-0 grade during vertical burning tests with the LOI of 27.3%. Jiao et al.[65] prepared a phenolic resin hollow microsphere (PHM). It was found that comparing TPU/4%PHM with pure TPU, the PHRR was reduced by 61.6%, the total smoke release (TSR) by 23.2%, and the CO production by 86.2%. The new organic synthetic flame retardant has the advantages of high flame retardancy efficiency, low addition amounts, and little impact on mechanical properties. Besides, it can also endow TPU with some other functionality. It is a kind of flame retardant additive with a wide research scope and has been widely concerned.

In this work, a novel flame retardant additive containing phosphoramide bonds based on diethylenetriamine and diphenyl phosphorochloridate was successfully synthesized and named DCPCD. The structure of DCPCD is characterized by Fourier transform infrared spectroscopy (FTIR), nuclear magnetic resonance (NMR), and X-ray photoelectron spectroscopy (XPS). Then, DCPCD was introduced into TPU with different ratios for preparing flame-retarded TPU composites. The effect of DCPCD on the flame retardancy of TPU composites was investigated. The decomposition path of DCPCD and its flame retardant mechanism in TPU composites were illustrated by analyzing the condensed phase products.

2. EXPERIMENTAL SECTION

2.1. Materials. Diethylenetriamine (AR, 99%), diphenyl phosphorochloridate (97%), and triethylamine (AR, 99%) were purchased from Shanghai Macklin Biochemical Co., Ltd. (Shanghai, China) and used without further purification. Tetrahydrofuran (THF, 99.9%, SuperDry, stabilized with 250 ppm BHT, J&KSeal) was obtained from Beijing J&K Scientific Co., Ltd. (Beijing, China). Ethanol (AR 99.7%) was provided by Beijing InnoChem Science & Technology Co., Ltd. (Beijing, China). Distilled water is made in our laboratory. TPU (9380A, Bayer) was purchased from Beijing Jinlis Technology Co., Ltd. (Beijing, China).

2.2. Synthesis of DCPCD. First, diphenyl phosphorochloridate (72.54 g, 0.27 mol) and triethylamine (38 mL, 0.27 mol) were dissolved in 165 mL of THF and transferred to the flask under nitrogen. Then, 60 mL of THF solution containing diethylenetriamine (9.29 g, 0.09 mol) was added dropwise into the flask by a constant-pressure dropping funnel at 0 °C under nitrogen. Afterward, the reaction mixture was stirred at 0 and 60 °C for 4 and 10 h sequentially. Next, triethylamine hydrochloride (TEA·HCl) was removed by suction filtration, and THF in the yellowish liquid product was removed by vacuum distillation at 60 °C to obtain the yellowish solid powder crude product. This is followed by washing repeatedly three times in the mixture of water and ethanol (water/ethanol = 1:1) to produce the white powder. Afterward, the white solid powder was dried in a vacuum oven at 80 °C for 5 h. The yield of the white solid powder (DCPCD) obtained is 83%. The synthesis route of DCPCD is shown in Scheme 1. FTIR (KBr, cm^{-1}): 3210 (−NH−), 2890 ($-CH_2-$), 1590, and 1490 (Ar-), 1310 (P═O), 1290 (P-NR_2), 1250 (P-NHR), 936 (P−O); ^1H NMR (700 MHz, DMSO-d6, ppm): 7.38 (m, 12H), 7.29−6.91 (m, 18H), 5.93 (m, 2H), 3.11−2.98 (m, 4H), 2.89 (m, 4H).

2.3. Preparation of Pure TPU and TPU Composites. Before processing, all ingredients were dried in a vacuum oven at 100 °C for 8 h. DCPCD and TPU with the formulation in Table 1 were first dry-mixed (shaken in a bag to combine), respectively, followed by melt-extruding with a twin-screw extruder (LHFS1-271822, Lab Tech Engineering Co., Ltd., Thailand). Ten heating zones were set at 150, 160, 170, 175, 185, 185, 185, 175, 170, and 165 °C, and the screw speed was set at 80 r/min. The specimens for different tests were molded at

Table 1. Formulations of Pure TPU and TPU/DCPCD Composites

samples	TPU(g)	DCPCD(g)
TPU	1000	0
TPU/1%DCPCD	990	10
TPU/3%DCPCD	970	30
TPU/6%DCPCD	940	60
TPU/9%DCPCD	910	90
TPU/12%DCPCD	880	120

https://doi.org/10.1021/acsomega.3c01464
ACS Omega 2023, 8, 18151−18164

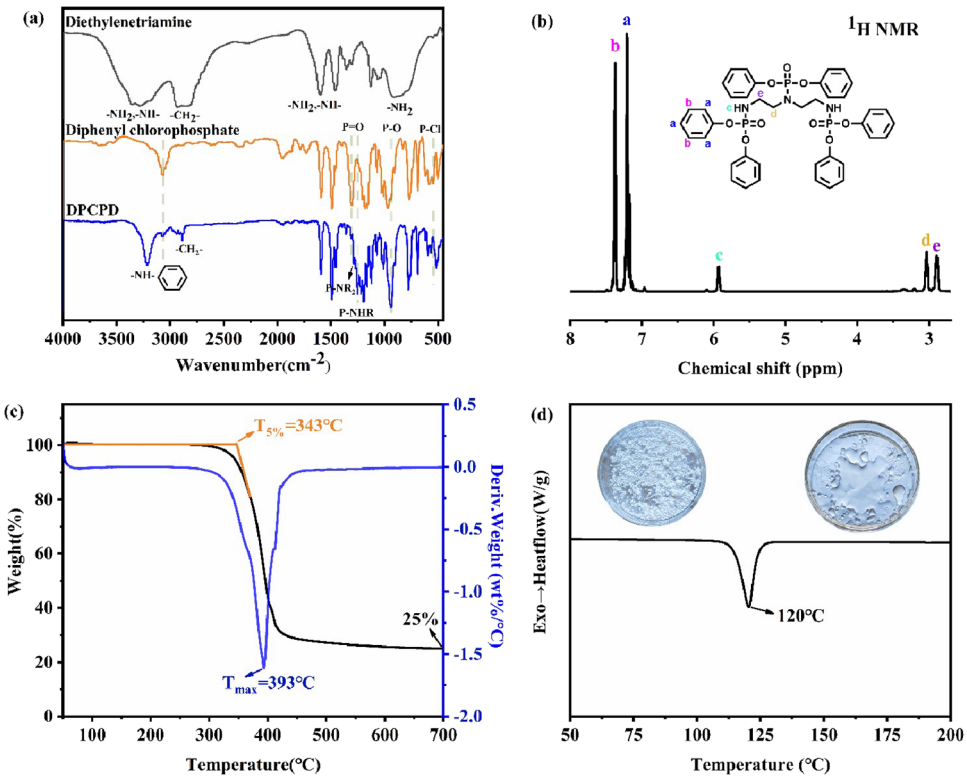

Figure 1. (a) FTIR spectra of DCPCD in 4000−500 cm^{-1}, (b) ^1H NMR spectrum of DCPCD, (c) TG and DTG curves of DCPCD under a N_2 atmosphere, and (d) DSC curve of DCPCD.

180 °C by a vertical injection molding machine (TY-400, Hangzhou Dayu Machinery Co., Ltd., China) and a vacuum-forming molding machine (VC-150-T-FTMO-3RT, Jiaxin Electronic Equipment Technology Co., Ltd., China).

2.4. Characterizations. Structural characterization: the chemical structure of DCPCD was characterized and verified by FTIR and ^1H NMR. FTIR spectra were scanned on a Nicolet iN10MX-type infrared spectrometer. ^1H NMR spectra were detected by a Bruker Avance III HD 700 MHz NMR spectrometer, by using dimethyl sulfoxide-d6 (DMSO) as the deuterated solvent.

The LOI values were measured via a 300800 LOI instrument (Concept Equipment Ltd., UK) according to ASTM D2863 with a sample dimension of 100.0 × 6.5 × 3.2 mm^3.

The vertical burning tests for the UL 94 combustion level were conducted on an FTT 0082 instrument (Fire Testing Technology, UK) with sample dimensions of 130 mm × 13 mm × 3.2 mm according to the ASTM D3801 testing procedure. Five specimens were tested for each sample.

Fire behavior was characterized on an FTT cone calorimeter (Fire Testing Technology, London, UK) according to ISO5660 under a 50 kW/m^2 external heat flux with a sample dimension of 100.0 × 100.0 × 3.2 mm^3. Time to ignition (TTI), total heat release (THR), TSR, and other typical parameters were collected and recorded synchronously, and the reported data were the average from three measurements.

The thermogravimetric (TG) analysis was performed using a Perkin-Elmer instrument STA8000 (Perkin Elmer, USA) thermogravimetric analyzer. About 8 mg of the sample was heated from 50 to 800 °C at the rate of 20 °C/min in a N_2 or air atmosphere. All tests were repeated two times.

Differential scanning calorimetry (DSC) test: The glass transition temperature (T_g) was detected under a nitrogen (N_2) atmosphere by using the Perkin-Elmer differential scanning calorimeter DSC 6000 (Perkin Elmer, USA). About 6 mg of the sample was quickly heated up to 250 °C and kept for 5 min to eliminate heat history, then cooled down to 30 °C at the rate of 20 °C/min and held at 30 °C for 5 min, and finally heated up to 250 °C at the rate of 20 °C/min.

The microscopic morphology of the residual char after the cone calorimeter test was observed on a Phenom ProX SEM (SEM, Phenom World, Holland) under vacuum conditions with a voltage of 10 kV.

XPS spectra were obtained on EscaLab Xi+ equipment (Thermo Scientific, America). The vacuum degree of the analysis chamber was 8×10^{-10} Pa, and the working voltage was 14.4 kV.

The Raman data were measured by a laser Raman spectrometer (Renishaw inVia plus, UK) at ambient temperature by a 532 nm laser.

The total transmittance spectra were measured in the range of 500−1500 nm using a UV−vis spectrophotometer (UV-3600, Shimadzu, Japan) with a sample thickness of 50.0 × 50.0 × 0.2 mm at room temperature.

The values of transmittance and haze were tested by a transmittance haze tester (WGT-S, Shanghai Precision Scientific Instrument Co., Ltd) according to the determination of the luminous transmittance and haze of transparent plastics standard (GB/T 2410-2008) with a sample thickness of 50.0 × 50.0 × 0.2 mm at room temperature; all tests were repeated five times.

3. RESULTS AND DISCUSSION

3.1. Synthesis and Characterization of DCPCD. DCPCD was obtained by the nucleophilic substitution reaction between the chlorine atom of diphenyl phosphorochloridate and

https://doi.org/10.1021/acsomega.3c01464
ACS Omega 2023, 8, 18151−18164

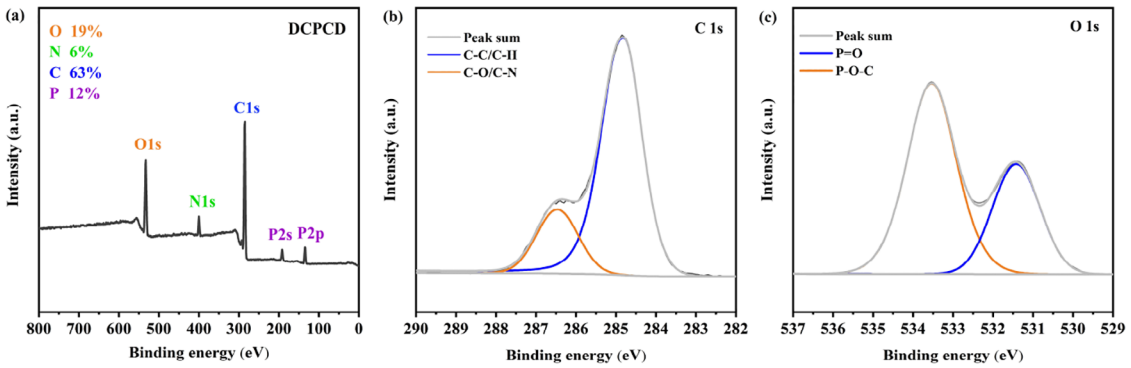

Figure 2. XPS full spectrum of DCPCD (a) and the C 1s (b) and O 1s (c) XPS high-resolution spectra of DCPCD.

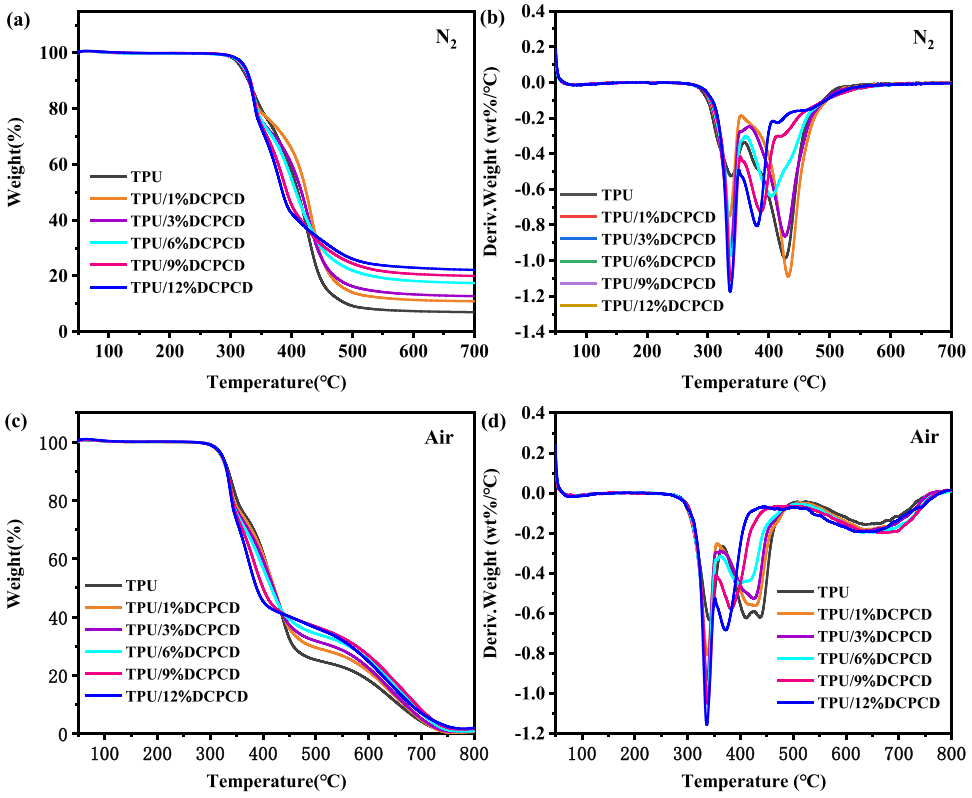

Figure 3. TG (a, c) and DTG (b, d) curves of pure TPU and TPU composites under a N_2 atmosphere and an air atmosphere.

the amino group of diethylenetriamine. The chemical structure and thermal behavior of DCPCD were identified by FTIR, ^{1}H NMR, XPS, TG, and DSC, which are shown in Figure 1.

The FTIR spectra of diethylenetriamine, diphenyl phosphorochloridate, and DCPCD are presented in Figure 1a. Comparing the FTIR spectra of DCPCD with diphenyl phosphorochloridate, it can be seen that the absorption peak of P−Cl (541 cm^{-1}) completely disappears in the spectra of DCPCD. It indicates that diphenyl phosphorochloridate and diethylenetriamine react completely. In addition, two absorption peaks belonging to $-NH_2$ (3360 and 3280 cm^{-1}) in diethylenetriamine disappeared in the spectrum of DCPCD. At the same time, compared with diphenyl phosphorochloridate, several peaks appear in the spectrum of DCPCD. The peak at 3210 cm^{-1} can be ascribed to the stretching vibration of −NH−, and the peak at 2890 cm^{-1} can be attributed to the stretching vibration of $-CH_2-$. In particular, the peaks at 1290 and 1250 cm^{-1} are designated to the stretching vibration of P-NR_2 and P-NHR, respectively.

As displayed in Figure 1b, the influence of the shielding effect of the hydrogen atom will reduce the chemical shift so that the peak at 2.89 ppm (marked by e) is assigned to the protons of $-CH_2-$ near the secondary amine, and the peak at 3.11−2.98 ppm (marked by d) corresponds to the protons of $-CH_2-$ near the tertiary amine. Moreover, the chemical shifts at 5.93 ppm (N−H protons, marked by c), 7.38 ppm, and 7.29−6.91 ppm (the protons on the monosubstituted benzene ring, marked by b and a) are also found in the ^{1}H NMR spectrum of DCPCD. In addition, the experimental proportion of the integral area according to different peaks is b:a:c:d:e = 11:18:2:4:4, which is consistent with the theoretical number of protons in different chemical environments. All the above results confirmed the chemical structure of DCPCD.

Figure 1c shows the TG and DTG (from 50 to 700 °C) curves of the flame retardant DCPCD under a nitrogen atmosphere. To

https://doi.org/10.1021/acsomega.3c01464
ACS Omega 2023, 8, 18151−18164

Table 2. Data of TG and DTG for Pure TPU and TPU/DCPCD Composites in N_2

samples	$T_{5\%}$, °C	T_{max1}, °C	T_{max2}, °C	residue at 700 °C, %	theoretical residue at 700 °C, %
TPU	317	339	425	7	7
TPU/1%DCPCD	320	336	432	11	7
TPU/3%DCPCD	320	337	427	13	8
TPU/6%DCPCD	321	339	405	18	8
TPU/9%DCPCD	323	338	388	20	9
TPU/12%DCPCD	324	337	381	22	9

gain more information, distinctive data such as the temperature of 5% weight loss ($T_{5\%}$), the temperature of the maximum degradation rate (T_{max}), and the char residue at 700 °C are marked in Figure 1c. As seen, the thermal degradation range of DCPCD occurs between 300 and 465 °C, the $T_{5\%}$ is 343 °C, and the T_{max} is 393 °C. After heating, the char residue at 700 °C is as high as 25 wt %. Figure 1d shows the DSC curve of the flame retardant DCPCD under a nitrogen atmosphere. The figure shows that the melting temperature (T_m) of DCPCD is 120 °C.

As depicted in Figure 2, DCPCD is investigated by XPS. It can be observed from Figure 2a that the DCPCD powder contains four kinds of elements, including C, O, N, and P. The experimental value of element contents listed in Figure 2a is consistent with the theoretical value calculated according to the structural formula of DCPCD. According to the XPS-peak differentiating analysis of C 1s (Figure 2b), the main peaks contain C−C or C−H (284.8 eV) and C−O or C−N (286.5 eV).[67] For the O 1s spectrum (Figure 2c), the peaks at 531.4 and 533.6 eV belong to the phosphorus−oxygen double bond (P═O) and single bond (P−O−C).[68] Hence, it can be proved that DCPCD is successfully synthesized.

3.2. Thermal Properties of Pure TPU and Flame Retardant TPU Composites. To explore the effect of DCPCD on the thermal properties of TPU, the thermal stability and T_g of TPU/DCPCD composites were studied by TG and DSC. The TG results of TPU and TPU/DCPCD composites under nitrogen and air atmospheres are shown in Figure 3. The detailed TG and DTG data are listed in Tables 2 and 3. There

Table 3. Data of TG and DTG for Pure TPU and TPU/DCPCD Composites in Air

samples	$T_{5\%}$, °C	T_{max1}, °C	T_{max2}, °C	residue at 700 °C, %
TPU	321	341	414	0.95
TPU/1%DCPCD	322	339	412	0.47
TPU/3%DCPCD	322	338	400	0.81
TPU/6%DCPCD	323	338	389	0.72
TPU/9%DCPCD	323	338	381	1.58
TPU/12%DCPCD	323	337	373	1.86

are two TPU decomposition stages under a nitrogen atmosphere. The first one is attributed to the degradation of the urethane bond of the TPU hard segments, and the main products at this stage are isocyanates, alcohols, amines, and carbon dioxide. The second stage is due to the thermal decomposition of the polyether polyol of the TPU soft segment.[1,69] The temperature at 5 wt % weight loss is regarded as the initial degradation temperature ($T_{5\%}$). It is referred from Figure 3a,b that pure TPU starts to degrade at 317 °C with T_{max1} at 339 °C and T_{max2} at 425 °C. $T_{5\%}$ of TPU composites is higher than that of pure TPU and increases slightly with the increase of the DCPCD weight because $T_{5\%}$ of DCPCD is higher than that of pure TPU. In addition, T_{max1} of TPU composites shows little change with the addition of DCPCD, and T_{max2} of TPU composites decreases significantly with the increase of the DCPCD weight, which may be caused by the decomposition of DCPCD at about 343 °C. Moreover, the char residues of TPU composites under nitrogen increase rapidly with the increased weight loading of DCPCD. No matter how much DCPCD is added, the experimental value of the char residues of TPU composites is much higher than the theoretical value, indicating that the addition of DCPCD promotes the formation of the char residues of TPU composites. It is shown in Figure 3c,d that there are three weight loss stages of TPU under air. The third decomposition stage of TPU composites corresponds to the further thermal oxidative decomposition of the carbon residue in the previous stage. It indicates that TPU/DCPCD composites form an organic carbon layer during the heating process and further decompose under high temperatures in the air. The char residues of TPU composites are still higher than that of pure TPU. The above test results show that the addition of DCPCD improves the thermal stability and charring ability of the TPU matrix.

The glass transition temperature (T_g) of pure TPU and TPU/DCPCD composites is shown in Figure 4a and Table 4. The T_g of pure TPU is 93.87 °C, and the T_g of TPU/DCPCD composites gradually move to high temperatures because of the hydrogen bond between DCPCD and TPU. The movement of the TPU molecular chain is limited due to hydrogen bonding (Figure 4d), so the T_g of TPU/DCPCD composites increase with the increase of the DCPCD content.[70,71] The improvement of T_g can bring better heat resistance to TPU composites. The hydrogen bond between DCPCD and TPU was characterized by FTIR. From Figure 4b, the characteristic C═O peak of TPU at about 1690−1740 cm^{-1} can be seen. A curve-fitting procedure based on the Gaussian distribution was used to study the change of the C═O groups with the addition of DCPCD, as shown in Figure 4c. The peak near 1700 cm^{-1} represents the hydrogen-bonded C═O groups, and the peak near 1732 cm^{-1} represents the free C═O groups. With the increase of DCPCD, the intensity of the peak for the free C═O groups decreases, whereas the intensity of the peak for the hydrogen-bonded C═O groups increases. The ratios of the peak area of hydrogen-bonded C═O bands to the peak area of the free C═O bands calculated by integral software gradually increase from 1.27:1 for pure TPU to 2.54:1 for TPU/12%DCPCD, demonstrating the formation of a large number of new hydrogen bonds between the free C═O groups of TPU and the N−H groups of DCPCD.

3.3. Flame Retardancy of Pure TPU and Flame Retardant TPU Composites. The flame retardancy of pure TPU and TPU/DCPCD composites was evaluated by the UL 94 vertical burning test and the LOI measurement, as displayed in Figure 5a. The digital photos of the moment when the ignition source is removed in the 10th s of the first ignition during the vertical burning test are illustrated in Figure 5b. Figure 5a shows that pure TPU is flammable, which shows the LOI value of

https://doi.org/10.1021/acsomega.3c01464
ACS Omega 2023, 8, 18151−18164

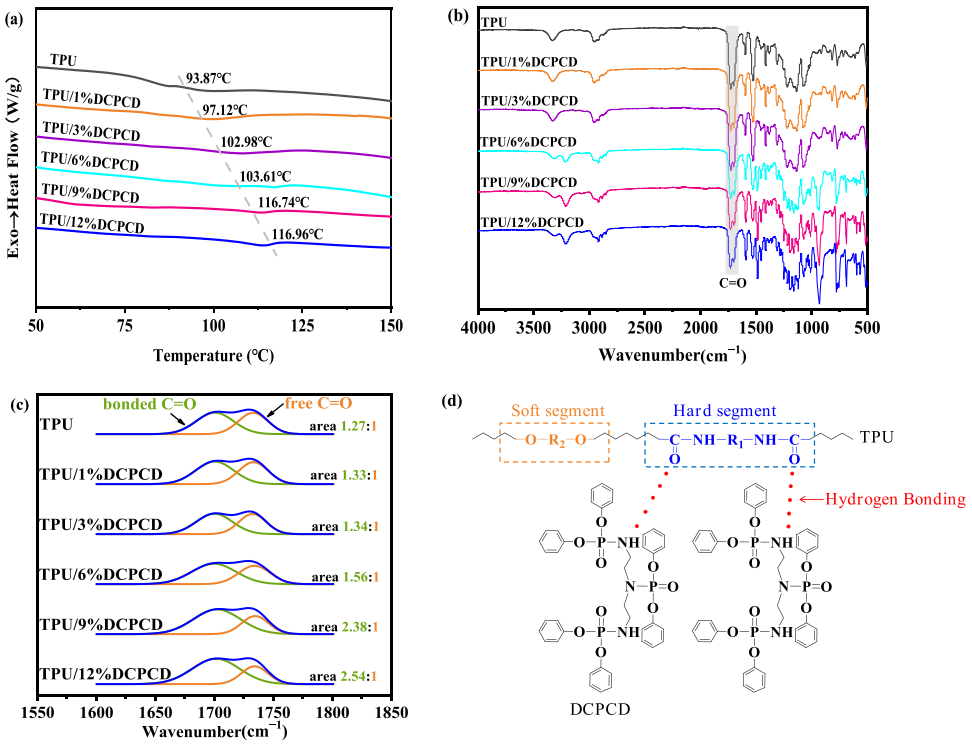

Figure 4. (a) Data of T_g for pure TPU and TPU/DCPCD composites in N_2, (b) infrared spectra of TPU and TPU/DCPCD composites, (c) curve-fitting results of the C═O stretching region, and (d) hydrogen bonding between TPU and DCPCD in the TPU/DCPCD composites.

Table 4. Curve-Fitting Results of the C═O Stretching Region and T_g

	hydrogen-bonded C═O		free C═O		DSC(N_2)
samples	wavenumber (cm^{-1})	area (%)	wavenumber (cm^{-1})	area (%)	T_g (°C)
TPU	1701	55.90	1733	44.10	93.87
TPU/1%DCPCD	1700	57.16	1733	42.84	97.12
TPU/3%DCPCD	1699	57.29	1732	42.71	102.98
TPU/6%DCPCD	1698	61.00	1731	39.00	103.61
TPU/9%DCPCD	1699	70.38	1731	29.62	116.74
TPU/12%DCPCD	1699	71.74	1731	28.26	116.96

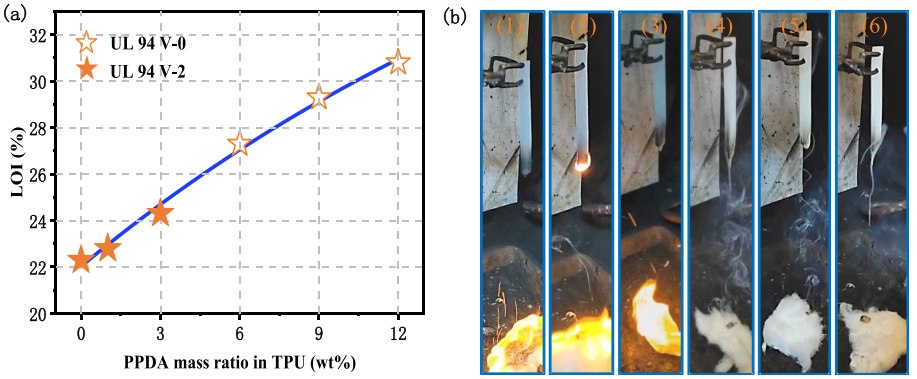

Figure 5. (a) UL 94 vertical burning test results and LOI values of pure TPU and TPU/DCPCD composites. (b) Digital photos of (1) TPU, (2) TPU/1%DCPCD, (3) TPU/3%DCPCD, (4) TPU/6%DCPCD, (5) TPU/9%DCPCD, and (6) TPU/12%DCPCD during the UL 94 vertical burning test.

22.3% and V-2 rating in the UL 94 vertical burning test, accompanied by severe melt dripping. Additionally, absorbent cotton was quickly ignited by molten drops, posing a severe secondary threat in actual fires. The LOI values of TPU/DCPCD composites gradually increase as the contents of DCPCD increase. When the amount of DCPCD is increased to 6%, the LOI value of TPU/6%DCPCD could reach 27.3%, passing the UL 94 V-0 rating. Although there was dripping, the absorbent cotton was not ignited. The LOI value of TPU/12% DCPCD raised to 30.8%, which is the highest among all the test samples. The combustion of the samples during the UL 94 vertical burning test can be observed in Figure 5b. It can be seen that after the first ignition, all samples dropped at the moment when the ignition source left. When the content of DCPCD is 1

https://doi.org/10.1021/acsomega.3c01464
ACS Omega 2023, 8, 18151−18164

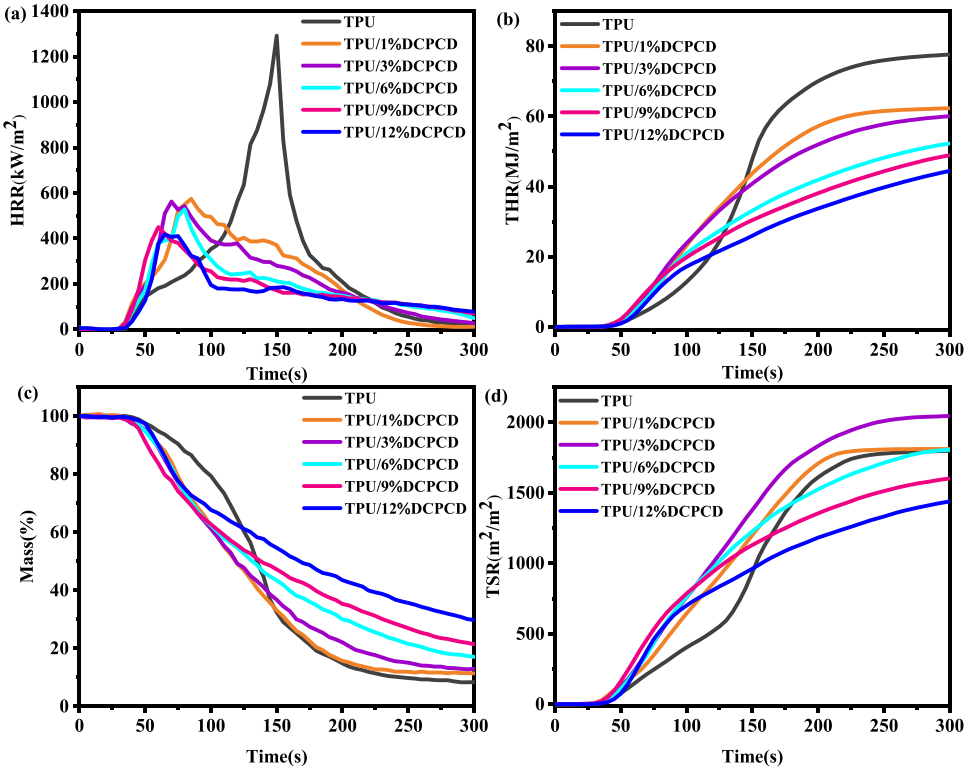

Figure 6. HRR (a), THR (b), mass (c), and TSR (d) curves of pure TPU and TPU/DCPCD composites.

Table 5. Cone Calorimeter Data of Pure TPU and TPU/DCPCD Composites

sample	TTI (S)	PHRR (kW/m^2)	THR (MJ/m^2)	av-EHC (MJ/kg)	av-MLR (g/s)	TSR (m^2/m^2)	av-COY (kg/kg)	av-CO_2Y (kg/kg)	residue char (%)	FPI ($s\ m^2\ kW^{-1}$)
TPU	32 ± 2	1292 ± 31	78 ± 5	17 ± 2	0.15 ± 0.02	1795 ± 12	0.04 ± 0.01	1.47 ± 0.05	8 ± 1	0.025
TPU/1%DCPCD	27 ± 2	574 ± 11	62 ± 1	16 ± 1	0.13 ± 0.01	1808 ± 10	0.04 ± 0.01	1.35 ± 0.02	11 ± 1	0.047
TPU/3%DCPCD	27 ± 1	562 ± 10	61 ± 1	16 ± 1	0.10 ± 0.01	2049 ± 13	0.05 ± 0.01	1.33 ± 0.02	12 ± 1	0.048
TPU/6%DCPCD	28 ± 1	528 ± 22	54 ± 2	15 ± 1	0.10 ± 0.01	1809 ± 11	0.06 ± 0.01	1.26 ± 0.03	16 ± 1	0.053
TPU/9%DCPCD	28 ± 2	449 ± 17	51 ± 3	15 ± 1	0.09 ± 0.02	1624 ± 10	0.06 ± 0.01	1.26 ± 0.03	19 ± 1	0.062
TPU/12%DCPCD	33 ± 1	417 ± 12	48 ± 2	15 ± 1	0.09 ± 0.02	1501 ± 13	0.06 ± 0.01	1.27 ± 0.02	25 ± 2	0.079

and 3%, the drops can ignite the absorbent cotton. When the DCPCD content is equal to or higher than 6%, the dripping of melt was reduced, and the absorbent cotton was not ignited. In addition, it is observed that the drops could remove flame and heat and inhibit combustion, making the samples self-extinguish.

The effect of DCPCD on the flame retardancy of TPU composites was further explored by cone calorimeter tests, and the result is shown in Figure 6 and Table 5. As shown in Figure 6a,b, it is worth noting that the PHRR of TPU can be reduced from 1292 to 574 kW/m^2 by adding only 1% DCPCD, and the THR decreases from 78 to 62 MJ/m^2, which drop by 55.6 and 20.5% compared with the PHRR and THR of pure TPU. With the increase of DCPCD, both the PHRR and THR decrease steadily, and the corresponding values of TPU/12%DCPCD are reduced by 67.7 and 38.5%, indicating that DCPCD effectively reduces the heat release of TPU during burning and has a positive effect in improving the fire safety of TPU.

As shown in Figure 6c, there is a little residual char left after the combustion of pure TPU. As the mass percentage of DCPCD is increased, there is a dramatic higher trend in the residue char and a sharp decreasing trend in the average mass loss rate (av-MLR), which demonstrates that DCPCD might give substrates improved charring capabilities.[72] Compared to pure TPU, the carbon residue of TPU/12%DCPCD increased by more than three times, which is consistent with the TG test results.

Smoke generated in the process of fire is also one of the main risk factors of fire. Figure 6d and Table 5 reveal the TSR curves and data of pure TPU and TPU composites. The TSR of pure TPU is 1795 m^2/m^2. With the addition of DCPCD, the TSR values increase first and then decrease, and the TSR value of the TPU/12%DCPCD composite declined to 1501 m^2/m^2, which is 16.4% lower than that of pure TPU. When the amount of DCPCD added is low, the protective effect of the carbon layer is weak, and some decomposition products enter the gas phase in the form of smoke, leading to the increase of the TSR. With a large additional amount of DCPCD, more high-quality carbon layers are formed, and more decomposition products remain in the condensed phase, resulting in the decline of the TSR.

The average effective heat of combustion (av-EHC) value reveals the burning degree of gas volatiles during combustion.[46] With the addition of DCPCD, the av-EHC of TPU composites gradually decreases. This result further explains that DCPCD can effectively delay the decomposition of the TPU matrix, and the inhibition will lead to incomplete combustion and reduce the heat release during combustion. With the increase of DCPCD addition, the average carbon monoxide yield (av-COY) gradually increases, and the av-CO_2Y gradually decreases,

https://doi.org/10.1021/acsomega.3c01464
ACS Omega 2023, 8, 18151−18164

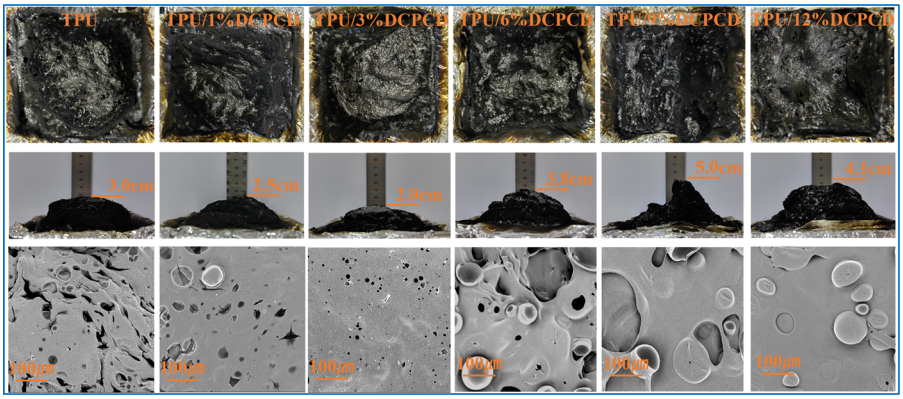

Figure 7. Digital photos and SEM images of the residual char for pure TPU and TPU/DCPCD composites after the cone calorimeter test.

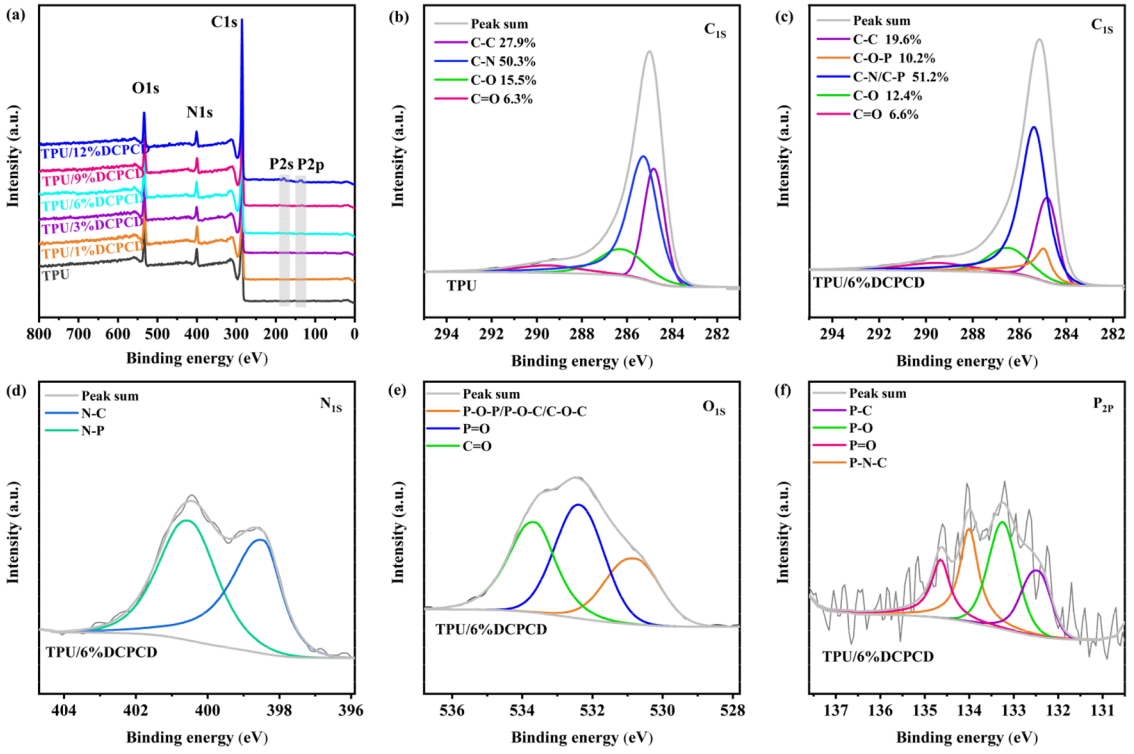

Figure 8. XPS full spectrum of the char residue of TPU and TPU/DCPCD composites (a). The C 1s XPS high-resolution spectra of the char residue of TPU (b) and TPU/6%DCPCD (c). N 1s, O 1s, and P 2p XPS high-resolution spectra of the char residue of TPU/6%DCPCD (d–f).

caused by less complete oxidation of the material during combustion, which illustrates that the addition of DCPCD can inhibit the combustion of materials. Fire performance index (FPI) (s m^2 kW^{-1}) is the ratio of TTI and the PHRR.[18] A lower FPI value means the time to catch flashover is shorter and the fire risk is higher. With the increase of DCPCD addition, the FPI values of TPU composites gradually increase, which indicates that TPU composites have a higher safety level than pure TPU.

3.4. Char Residue Analysis. DCPCD participated in the carbonization process of TPU, which might not only increase the quantity of the residual char but also improve the quality of the residual char. Digital photos and SEM micrographs of the residues obtained from the cone calorimetry test for TPU and TPU/DCPCD are shown in Figure 7. From the macro residue digital photos, it can be seen that compared with pure TPU, when the addition of DCPCD is greater than or equal to 6%, the expansion degree of the residue of TPU/DCPCD composites is significantly increased. The SEM micrographs show that the char residue of pure TPU is broken and full of cracks and holes. When 1 wt % DCPCD is added, the cracked holes of the char layer become smaller. When 6 wt % DCPCD is added, the char residue of the TPU/DCPCD composite is further reduced, and char foaming is formed. Among all the samples, the residue of TPU/12%DCPCD is the most complete and compact, and char foaming can be observed.

The elemental compositions of the char residues for TPU and TPU/DCPCD composites were further analyzed by XPS tests, and the corresponding spectra are presented in Figure 8. As shown in Figure 8a and Table 6, the elemental compositions of the char residue for TPU/DCPCD composites were C, O, N, and P, and the contents of P increased with the addition of DCPCD. Figure 8b,c displays XPS-peak differentiating analysis of C 1s for TPU and TPU/6%DCPCD. The C 1s peaks of the char residue of TPU at 284.8, 285.3, 286.3, and 289.4 eV are ascribed to the C−C, C−N, C−O, and C═O. For TPU/6% DCPCD, the peak area at 285.3 eV corresponds to the C−N/

https://doi.org/10.1021/acsomega.3c01464
ACS Omega 2023, 8, 18151−18164

Table 6. P Content (%) of TPU Composites and Char Layer of TPU Composites after Cone Calorimetry

	P content (%)	
sample	TPU composites	char layer of TPU composites after cone calorimetry
TPU	0	0
TPU/1%DCPCD	0.12	0
TPU/3%DCPCD	0.35	0.34
TPU/6%DCPCD	0.70	0.64
TPU/9%DCPCD	1.05	0.92
TPU/12%DCPCD	1.40	1.31

C−P bond, which increased because the char residue of TPU/6%DCPCD contains C−P. In addition, TPU/6%DCPCD has a new peak at 285.0 eV that is ascribed to the C−O−P.[64,68,73,74] Figure 8d−f shows the XPS-peak differentiating analysis of O 1s, N 1s, and P 2p of the char residue for TPU/6%DCPCD. The N 1s peaks of the char residue of TPU/6%DCPCD at 398.6 and 400.6 eV are ascribed to the N−C and N−P. For the O 1s spectrum, the peaks at 530.9 eV belong to the phosphorus−oxygen single bond or carbon−oxygen single bond from P−O−P, P−O−C, or C−O−C groups. The peaks at 532.4 and 533.7 eV belong to the phosphorus−oxygen double bond (P═O) and carbon−oxygen double bond (C═O). In the high-resolution P 2p XPS spectrum, the fitting analysis presents four deconvoluted peaks at 132.5, 133.3, 134.0, and 134.7 eV corresponding to P−C, P−O, P−N−C, and P═O bonds, respectively.[68,75,76] Combined with the above analysis, the results indicate that DCPCD could promote the formation of a phosphorus-containing carbon layer with higher cross-linking and strength in the TPU matrix during burning (Figure 9).

To further illuminate the flame retardant mechanism of TPU/DCPCD composites, the char residues of TPU and TPU/DCPCD composites were analyzed by Raman measurement, as exhibited in Figure 10. Two distinctive peaks, the D peak and the G peak, are visible at 1360 and 1590 cm^{-1}, respectively. Typically, the G peak relates to the structured graphite structure, whereas the D peak stands for the disordered graphite structure; the degree of graphitization of the char residue is often represented by the area ratio of the D peak to the G peak (I_D/I_G). If the I_D/I_G value is low, it means that the char residue has a high degree of graphitization and is dense and solid.[52,77] As displayed in Figure 10, the pure TPU shows a high I_D/I_G value (3.04). With the increase of DCPCD addition, the I_D/I_G ratios of TPU composites decrease gradually. When the additional amount of DCPCD is 12 wt %, the I_D/I_G value of TPU composites decreases to 2.84, which is the lowest. It indicates that the graphitization degree of char residues is improved after the addition of DCPCD.

3.5. Transparency Analysis. Transparency is an inherent excellent property of TPU materials. In many application fields of TPU, transparency is highly required, such as electronic and electrical enclosures, highly transparent adhesives, and film materials. However, higher flame retardancy is often at the expense of transparency. It is difficult to achieve high flame retardancy while maintaining the transparency of TPU. During the experiment, it was observed that the addition of DCPCD had little effect on the transparency of TPU. It can be seen from Figure 11 that the plastic pellets of TPU and TPU/DCPCD composites obtained by twin-screw extrusion granulation are all transparent. Moreover, the pictures under the pure TPU and TPU composite films can be seen clearly, which indicates that DCPCD almost has no influence on transparency.

In order to quantitatively characterize the influence of DCPCD addition on the transparency of TPU, UV−vis spectroscopy, transmittance, and haze tester are introduced.[78,79] As is shown in Figure 12a, in the wavelength range of 500−1500 nm, the total transmittance of pure TPU is from 75 to 85%. When the additional amount of DCPCD is 1 and 3 wt %, there is no effect on the total transmittance of TPU composites. Even 1 wt % DCPCD can slightly improve the transparency of TPU. The total transmittance of the TPU/6%DCPCD composite is from 51 to 78%, which increased with the increase of wavelength. TPU with 9 wt % DCPCD shows similar transmittance as that of TPU/6%DCPCD in the high-wavelength range, which decreases slightly in the low-wavelength range. When the amount of DCPCD is increased to 12 wt %, the total transmittance is greatly affected. The transmittance and haze test results are shown in Figure 12b. With the increase of the amount of DCPCD added, the transmittance first increases and then decreases. When the additional amount of DCPCD is 1 and 3 wt %, compared with pure TPU, the haze

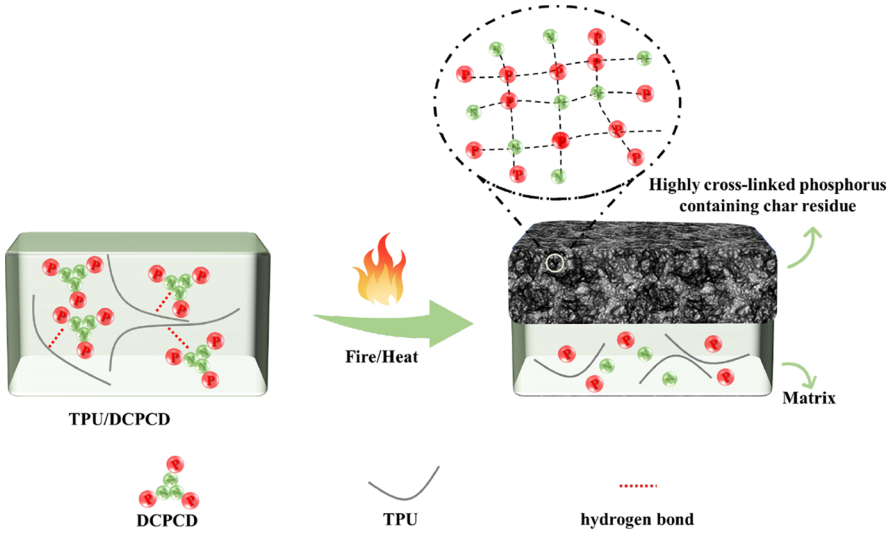

Figure 9. Possible flame retardant mechanism of TPU/DCPCD.

https://doi.org/10.1021/acsomega.3c01464
ACS Omega 2023, 8, 18151−18164

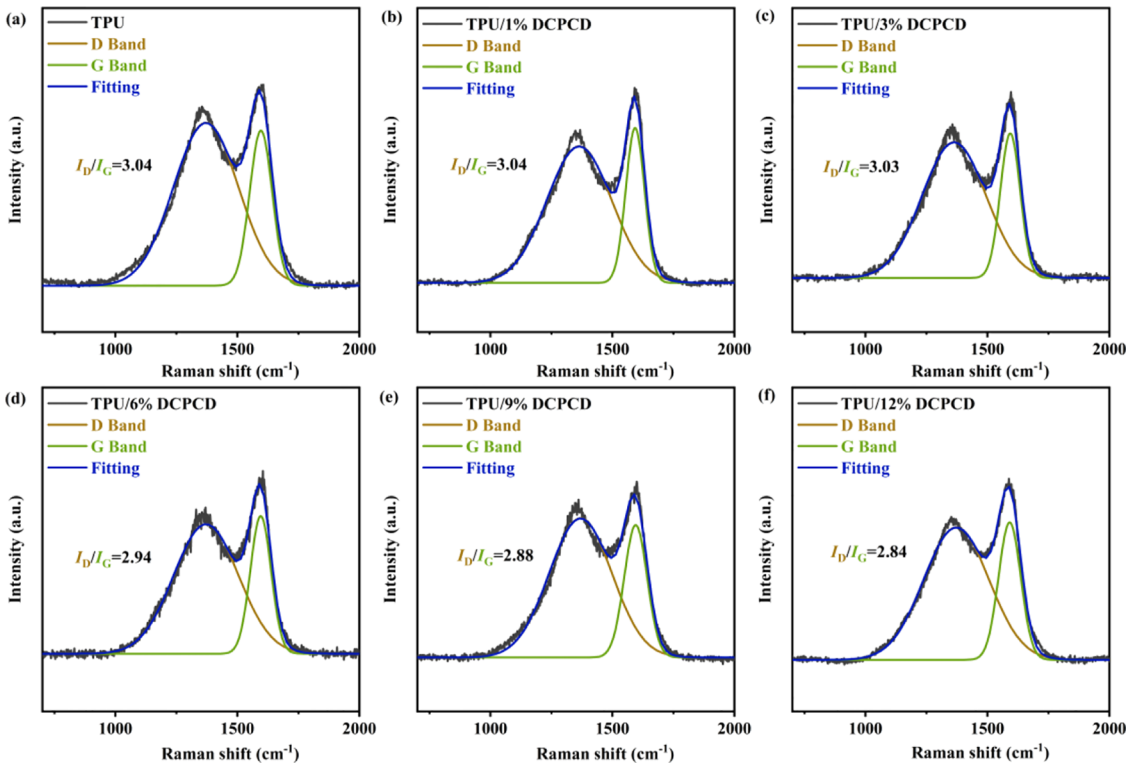

Figure 10. Raman spectral curves of char residues of pure TPU and TPU/DCPCD composites: (a) TPU, (b) TPU/1%DCPCD, (c) TPU/3% DCPCD, (d) TPU/6%DCPCD, (e) TPU/9%DCPCD, and (f) TPU/12%DCPCD.

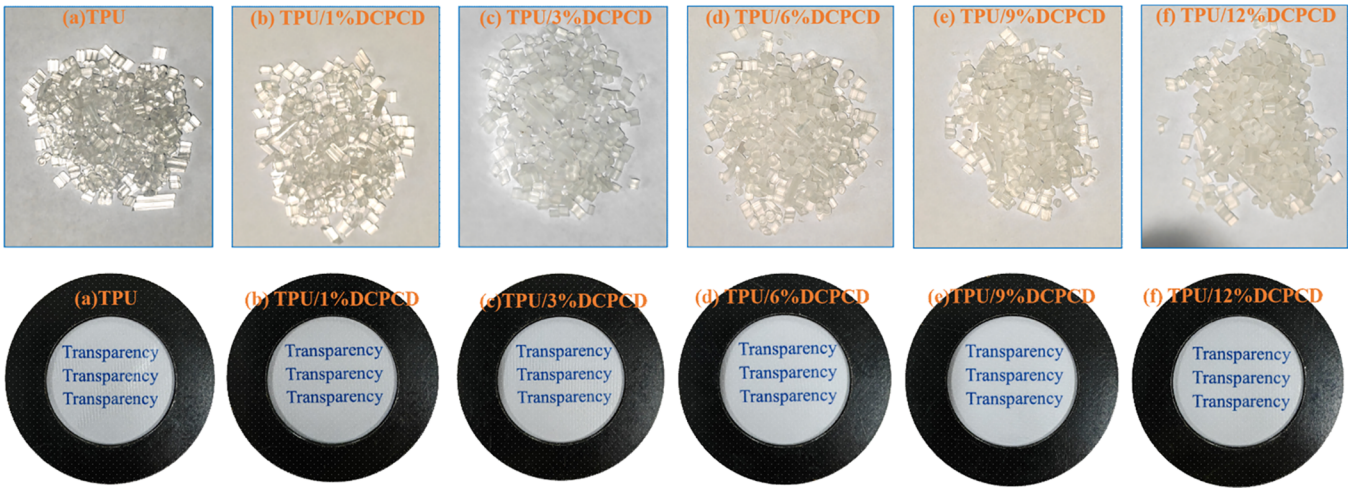

Figure 11. Digital photos of the pellets of pure TPU and TPU/DCPCD composites by twin-screw extrusion and pure TPU and TPU/DCPCD composite films under ambient light: (a) TPU, (b) TPU/1%DCPCD, (c) TPU/3%DCPCD, (d) TPU/6%DCPCD, (e) TPU/9%DCPCD, and (f) TPU/12%DCPCD.

decreases from 70 to 60%. When the addition of DCPCD is greater than 3 wt %, the haze of the TPU composite shows little change with the increase of the amount of DCPCD, which is consistent with pure TPU.

4. CONCLUSIONS

A kind of TPU composite simultaneously possessing excellent flame retardancy and transparency was obtained by adding a novel flame retardant additive (DCPCD) containing phosphoramide bonds, which was synthesized through diethylenetriamine and diphenyl phosphorochloridate. The chemical structure of DCPCD was successfully confirmed by FTIR, ^{1}H NMR, and XPS. The addition of DCPCD enhanced the char yield at 700 °C. With the incorporation of 6 wt % DCPCD, the UL 94 V-0 rating and the LOI value as high as 27.3% were achieved. The cone calorimetry test showed that the values of PHRR and THR were reduced after the incorporation of DCPCD. Compared with pure TPU, the PHRR and THR of the TPU/1%DCPCD composite were effectively reduced by 55.6 and 20.5%, and those for the TPU/6%DCPCD composite were further dramatically decreased by 59.1 and 30.8%. Meanwhile, the char residues of TPU with 6.0 wt % DCPCD increased by 100% from 8.0 wt % (pure TPU) to 16.0 wt %. Besides, TPU/6% DCPCD showed compact and continuous char layers, which

https://doi.org/10.1021/acsomega.3c01464
ACS Omega 2023, 8, 18151−18164

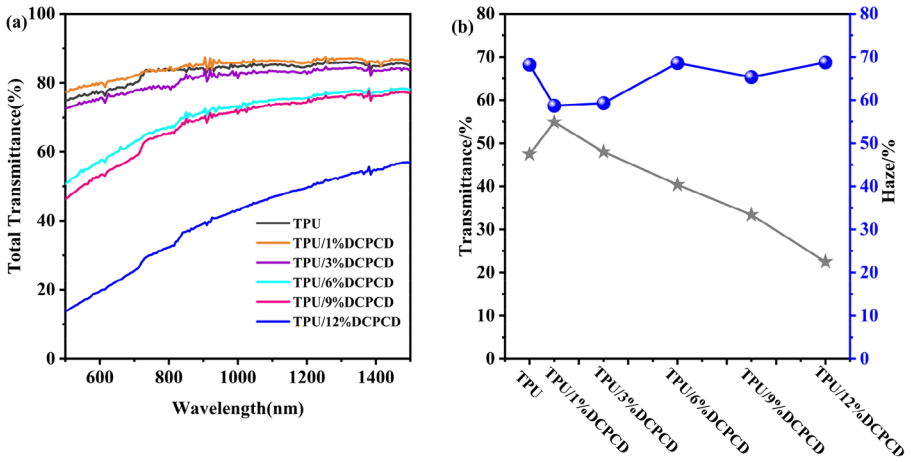

Figure 12. (a) Total transmittance (UV−vis spectrophotometer) and (b) transmittance and haze (transmittance haze tester) of TPU composite films.

function as a barrier to retard the combustion process. Raman spectroscopy suggested that DCPCD contributed to the formation of more stable char layers. SEM results showed that the presence of DCPCD caused obvious intumescence, which verified the condense phase flame retardant mechanism. The char residue of TPU/DCPCD composites after cone calorimetry was detected by XPS technology. XPS exhibited that DCPCD promoted the formation of a phosphorus-containing char layer with high cross-linking and strength in the TPU matrix after burning. In addition, the transmittance of TPU/DCPCD composites remained at a high level when the additional amount of DCPCD is less than 6 wt %. The haze of TPU composites shows little change with the increase of the amount of DCPCD, which is consistent with pure TPU. To sum up, DCPCD endowed TPU with high fire safety, and also the transparency was largely retained.

AUTHOR INFORMATION

Corresponding Author

Yajun Chen − *School of Chemistry and Materials Engineering, Beijing Technology and Business University, Beijing 100048, China; China Light Industry Engineering Technology Research Center of Advanced Flame Retardants, Beijing 100048, China; Petroleum and Chemical Industry Engineering Laboratory of Non-halogen Flame Retardants for Polymers, Beijing 100048, China;* orcid.org/0000-0002-3082-2078; Phone: 0086-10-68983954; Email: chenyajun@th.btbu.edu.cn

Authors

Mengqi Li − *School of Chemistry and Materials Engineering, Beijing Technology and Business University, Beijing 100048, China; China Light Industry Engineering Technology Research Center of Advanced Flame Retardants, Beijing 100048, China; Petroleum and Chemical Industry Engineering Laboratory of Non-halogen Flame Retardants for Polymers, Beijing 100048, China*

Zimeng Kong − *School of Chemistry and Materials Engineering, Beijing Technology and Business University, Beijing 100048, China; China Light Industry Engineering Technology Research Center of Advanced Flame Retardants, Beijing 100048, China; Petroleum and Chemical Industry Engineering Laboratory of Non-halogen Flame Retardants for Polymers, Beijing 100048, China*

Zhe Sun − *School of Chemistry and Materials Engineering, Beijing Technology and Business University, Beijing 100048, China; China Light Industry Engineering Technology Research Center of Advanced Flame Retardants, Beijing 100048, China; Petroleum and Chemical Industry Engineering Laboratory of Non-halogen Flame Retardants for Polymers, Beijing 100048, China*

Lijun Qian − *School of Chemistry and Materials Engineering, Beijing Technology and Business University, Beijing 100048, China; China Light Industry Engineering Technology Research Center of Advanced Flame Retardants, Beijing 100048, China; Petroleum and Chemical Industry Engineering Laboratory of Non-halogen Flame Retardants for Polymers, Beijing 100048, China;* orcid.org/0000-0002-8847-4934

Complete contact information is available at: https://pubs.acs.org/10.1021/acsomega.3c01464

Notes

The authors declare no competing financial interest.

ACKNOWLEDGMENTS

This work was financially supported by the National Natural Science Foundation (Nos. 22175006 and 51973006).

REFERENCES

(1) Wan, L.; Deng, C.; Chen, H.; Zhao, Z.; Huang, S.; Wei, W.; Yang, A.; Zhao, H.; Wang, Y. Flame-Retarded Thermoplastic Polyurethane Elastomer: From Organic Materials to Nanocomposites and New Prospects. *Chem. Eng. J.* **2021**, *417*, No. 129314.

(2) Petrovíc, Z.; Ferguson, J. Polyurethane Elastomers. *Prog. Polym. Sci.* **1991**, 695−836.

(3) Cooper, S.; Tobolsky, A. Properties of Linear Elastomeric Polyurethanes. *J. Appl. Polym. Sci.* **1966**, *10*, 1837−1844.

(4) Frontini, P.; Rink, M.; Pavan, A. Development of Polyurethane Engineering Thermoplastics. II. Structure and Properties. *J. Appl. Polym. Sci.* **1993**, *48*, 2023−2032.

(5) Eberlein, R.; Fukada, Y.; Pasieka, L. Fatigue Life Analysis of Solid Elastomer-Like Polyurethanes. *Adv. Polym. Sci.* **2020**, *286*, 179−202.

(6) Chen, T.; Xie, Y.; Wang, Z.; Lou, J.; Liu, D.; Xu, R.; Cui, Z.; Li, S.; Panahi-Sarmad, M.; Xiao, X. Recent Advances of Flexible Strain Sensors Based on Conductive Fillers and Thermoplastic Polyurethane Matrixes. *ACS Appl. Polym. Mater.* **2021**, *3*, 5317−5338.

(7) Toshiaki, N.; Takeshi, Y.; Shibata, K.; Ito, Y.; Kazuo, H. Wear Behavior of Thermoplastic Urethane for the Outer Soles of Spike Shoes. *Wear* **2022**, *490-491*, No. 204105.

(8) Shou, T.; Hu, S.; Wu, Y.; Tang, X.; Fu, G.; Zhao, X.; Zhang, L. Biobased and Recyclable Polyurethane for Room-Temperature Damp-

ing and Three-Dimensional Printing. *ACS Omega* **2021**, *6*, 30003−30011.
(9) Yoo, Y.; Cho, K. Development of Cost-Effective LoT Module-Based Pipe Classification System for Flexible Manufacturing System of Painting Process of High-Pressure Pipe. *Int. J. Adv. Manuf. Technol.* **2022**, *119*, 5453−5466.
(10) Zhou, Z.; Wang, K.; Lin, K.; Wang, Y.; Li, J. Influence of Characteristics of Thermoplastic Polyurethane on Graphene-Thermoplastic Polyurethane Composite Film. *Micromachines* **2021**, *12*, 129.
(11) Xu, Y.; Xu, Y.; Zhu, W.; Zhang, W.; Gao, Q.; Li, J. Improve the Performance of Soy Protein-Based Adhesives by a Polyurethane Elastomer. *Polymers* **2018**, *10*, 1016.
(12) Chen, S.; Lee, K.; Chang, C.; Hsu, T.; Feng, C. Using Gas Counter Pressure and Combined Technologies for Microcellular Injection Molding of Thermoplastic Polyurethane to Achieve High Foaming Qualities and Weight Reduction. *Polymers* **2022**, *14*, 2017.
(13) Zhao, B.; Qian, X.; Qian, Y.; Fan, J.; Feng, Y.; Duo, Y.; Zhang, H. Preparation of High-Performance Microfiber Synthetic Leather Base Using Thermoplastic Polyurethane/Sulfonated Polysulfone Electrospun Nanofibers. *Text. Res. J.* **2018**, *89*, 2813−2820.
(14) Yu, C.; Lai, C.; Wang, F.; Liu, L.; Liang, W.; Wu, C.; Chiu, J.; Liu, H.; Hsiao, H.; Chen, C. Fabrication of Thermoplastic Polyurethane (TPU)/Thermoplastic Amide Elastomer (TPAE) Composite Foams with Supercritical Carbon Dioxide and Their Mechanical Properties. *J. Manuf. Process.* **2019**, *48*, 127−136.
(15) Wang, X.; Geng, T.; Han, J.; Liu, C.; Shen, C.; Turng, L.; Yang, H. Effects of Nanoclays on the Thermal Stability and Flame Retardancy of Microcellular Thermoplastic Polyurethane Nanocomposites. *Polym. Compos.* **2018**, *39*, E1429−E1440.
(16) Toldy, A.; Harakály, G.; Szolnoki, B.; Zimonyi, E.; Marosi, G. Flame Retardancy of Thermoplastics Polyurethanes. *Polym. Degrad. Stab.* **2012**, *97*, 2524−2530.
(17) Liu, L.; Xu, Y.; Li, S.; Xu, M.; He, Y.; Shi, Z.; Li, B. A Novel Strategy for Simultaneously Improving the Fire Safety, Water Resistance and Compatibility of Thermoplastic Polyurethane Composites Through the Construction of Biomimetic Hydrophobic Structure of Intumescent Flame Retardant Synergistic System. *Compos. B Eng.* **2019**, *176*, No. 107218.
(18) Ji, X.; Chen, D.; Wang, Q.; Shen, J.; Guo, S. Synergistic Effect of Flame Retardants and Carbon Nanotubes on Flame Retarding and Electromagnetic Shielding Properties of Thermoplastic Polyurethane. *Compos. Sci. Technol.* **2018**, *163*, 49−55.
(19) Naik, A.; Fontaine, G.; Bellayer, S.; Bourbigot, S. Salen Based Schiff Bases to Flame Retard Thermoplastic Polyurethane Mimicking Operational Strategies of Thermosetting Resin. *RSC Adv.* **2015**, *5*, 48224−48235.
(20) Jiao, C.; Zhang, Y.; Li, S.; Chen, X. Flame Retardant Effect of 1-Aminoethyl-3-Methylimidazolium Hexafluorophosphate in Thermoplastic Polyurethane Elastomer. *J. Therm. Anal. Calorim.* **2020**, *145*, 173−184.
(21) Lee, S.; Cyriac, A.; Jeon, J.; Lee, B. Preparation of Thermoplastic Polyurethanes Using in Situ Generated Poly(Propylene Carbonate)-Diols. *Polym. Chem.* **2012**, *3*, 1215−1220.
(22) Niu, X.; Nie, Z.; Wang, G. Preparation, Flame Retardancy, and Thermal and Mechanical Properties of Polyurethane Containing Phosphonated Bisphenol-A Units. *Fire Mater.* **2018**, *42*, 933−945.
(23) Lligadas, G.; Ronda, J.; Galià, M.; Cádiz, V. Novel Silicon-Containing Polyurethanes from Vegetable Oils as Renewable Resources Synthesis and Properties. *Biomacromolecules* **2006**, *7*, 2420−2426.
(24) Xu, W.; Ren, M.; Liu, L. Synthesis and Characterization of Novel Phosphorus-Containing Polyurethane Elastomers. *Asian J. Chem.* **2014**, *26*, 1331−1333.
(25) Xu, W.; Lu, B.; Hu, Y.; Song, L.; Nie, S. Synthesis and Characterization of Novel Fluorinated Polyurethane Elastomers Based on 2,2-Bis[4-(4-Amino-2-Trifluoromehyloxyphenyl) Phenyl]propane. *Polym. Adv. Technol.* **2012**, *23*, 877−883.
(26) Chen, X.; Zhang, X.; Wang, Y.; Zhang, X.; Jiao, C. Synergistic Fire Safety Improvement Between Oyster Shell Powder and Ammonium Polyphosphate in TPU Composites. *Polym. Adv. Technol.* **2019**, *30*, 1564−1575.
(27) Wei, Z.; Chen, X.; Jiao, C. Thermal Degradation and Flame Retardancy of Fumaric Acid in Thermoplastic Polyurethane Elastomer. *Polym. Adv. Technol.* **2019**, *30*, 475−482.
(28) Kanbur, Y.; Tayfun, U. Development of Multifunctional Polyurethane Elastomer Composites Containing Fullerene: Mechanical, Damping, Thermal, and Flammability Behaviors. *J. Elastom. Plast.* **2018**, *51*, 262−279.
(29) Ma, Z.; Meng, D.; Zhang, Z.; Wang, Y. Synergistic Effect of Green Phosphorus-Containing Bio-Based Material and Two-Dimensional Layered Material Composite on Flame-Retardant Property of Polyvinyl Alcohol. *Thermochim. Acta* **2022**, *707*, No. 179118.
(30) Zhu, M.; Zhang, Y.; Sheng, H.; Wang, B.; Hu, Y. Effect Carbon Black Microencapsulated Ammonium Polyphosphate on the Flame Retardancy and Mechanical Properties of Polyurethane Composites. *Polym. Plast. Technol. Mater.* **2019**, *59*, 83−94.
(31) Qian, Y.; Qiao, P.; Li, L.; Han, H.; Zhang, H.; Chang, G. Hydrothermal Synthesis of Lanthanum-Doped MgAl-Layered Double Hydroxide/Graphene Oxide Hybrid and Its Application as Flame Retardant for Thermoplastic Polyurethane. *Adv. Polym. Technol.* **2020**, *2020*, 1−10.
(32) Wang, D.; Guo, J.; Su, M.; Sun, J.; Zhang, S.; Yang, W.; Gu, X.; Li, H. The Application of a Novel Char Source from Petroleum Refining Waste in Flame Retardant Thermoplastic Polyurethane. *Polym. Eng. Sci.* **2020**, *60*, 1029−1034.
(33) Savas, L.; Hacioglu, F.; Hancer, M.; Dogan, M. Flame Retardant Effect of Aluminum Hypophosphite in Heteroatom-Containing Polymers. *Polym. Bull.* **2019**, *77*, 291−306.
(34) Chen, X.; Ma, C.; Jiao, C. Enhancement of Flame-Retardant Performance of Thermoplastic Polyurethane with the Incorporation of Aluminum Hypophosphite and Iron-Graphene. *Polym. Degrad. Stab.* **2016**, *129*, 275−285.
(35) Xiao, S.; Chen, M.; Dong, L.; Deng, C.; Chen, L.; Wang, Y. Thermal Degradation, Flame Retardance and Mechanical Properties of Thermoplastic Polyurethane Composites Based on Aluminum Hypophosphite. *Chin. J. Polym. Sci.* **2013**, *32*, 98−107.
(36) Liu, X.; Guo, J.; Tang, W.; Li, H.; Gu, X.; Sun, J.; Zhang, S. Enhancing the Flame Retardancy of Thermoplastic Polyurethane by Introducing Montmorillonite Nanosheets Modified with Phosphorylated Chitosan. *Compos. A Appl. Sci. Manuf.* **2019**, *119*, 291−298.
(37) Zhou, Q.; Gong, K.; Zhou, K.; Zhao, S.; Shi, C. Synergistic Effect Between Phosphorus Tailings and Aluminum Hypophosphite in Flame-Retardant Thermoplastic Polyurethane Composites. *Polym. Adv. Technol.* **2019**, *30*, 2480−2487.
(38) Chen, X.; Ma, C.; Jiao, C. Synergistic Effects Between Iron-Graphene and Ammonium Polyphosphate in Flame-Retardant Thermoplastic Polyurethane. *J. Therm. Anal. Calorim.* **2016**, *126*, 633−642.
(39) Liu, L.; Zhao, X.; Ma, C.; Chen, X.; Li, S.; Jiao, C. Smoke Suppression Properties of Carbon Black on Flame Retardant Thermoplastic Polyurethane Based on Ammonium Polyphosphate. *J. Therm. Anal. Calorim.* **2016**, *126*, 1821−1830.
(40) Liu, C.; Zong, R.; Chen, H.; Wang, J.; Wu, C. Comparative Study of Toxicity for Thermoplastic Polyurethane and Its Flame-Retardant Composites. *J. Thermoplast. Compos. Mater.* **2018**, *32*, 1393−1407.
(41) Wu, Q.; Liu, Y.; Han, Z.; Su, M.; Sun, J.; Zhang, S.; Gu, X.; Li, H. Surface Modification of Bamboo Fibers by Diammonium Phosphate and Their Applications in Flame Retardant Thermoplastic Polyurethane. *J. Appl. Polym. Sci.* **2021**, *138*, No. e50606.
(42) Sut, A.; Metzsch-Zilligen, E.; Großhauser, M.; Pfaendner, R.; Schartel, B. Synergy Between Melamine Cyanurate, Melamine Polyphosphate and Aluminum Diethylphosphinate in Flame Retarded Thermoplastic Polyurethane. *Polym. Test.* **2019**, *74*, 196−204.
(43) Sut, A.; Metzsch-Zilligen, E.; Großhauser, M.; Pfaendner, R.; Schartel, B. Rapid Mass Calorimeter as a High-Throughput Screening Method for the Development of Flame-Retarded TPU. *Polym. Degrad. Stab.* **2018**, *156*, 43−58.

https://doi.org/10.1021/acsomega.3c01464
ACS Omega 2023, 8, 18151−18164

(44) Wilke, A.; Langfeld, K.; Ulmer, B.; Andrievici, V.; Hörold, A.; Limbach, P.; Bastian, M.; Schartel, B. Halogen-Free Multicomponent Flame Retardant Thermoplastic Styrene-Ethylene-Butylene-Styrene Elastomers Based on Ammonium Polyphosphate-Expandable Graphite Synergy. *Ind. Eng. Chem. Res.* **2017**, *56*, 8251−8263.
(45) Lai, X.; Zeng, X.; Li, H.; Liao, F.; Zhang, H.; Yin, C. Preparation and Properties of Flame Retardant Polypropylene with an Intumescent System Encapsulated by Thermoplastic Polyurethane. *J. Macromol. Sci. B* **2011**, *51*, 35−47.
(46) Ozcelik, G.; Elcin, O.; Guney, S.; Erdem, A.; Hacioglu, F.; Dogan, M. Flame-Retardant Features of Various Boron Compounds in Thermoplastic Polyurethane and Performance Comparison with Aluminum Trihydroxide and Magnesium Hydroxide. *Fire Mater.* **2022**, *46*, 1020−1033.
(47) Wang, N.; Li, L.; Xu, Y.; Zhang, K.; Chen, X.; Wu, H. Synergistic Effects of Red Phosphorus Masterbatch with Expandable Graphite on the Flammability and Thermal Stability of Polypropylene/Thermoplastic Polyurethane Blends. *Polym. Polym. Compos.* **2019**, *28*, 209−219.
(48) Guler, T.; Tayfun, U.; Bayramli, E.; Dogan, M. Effect of Expandable Graphite on Flame Retardant, Thermal and Mechanical Properties of Thermoplastic Polyurethane Composites Filled with Huntite&Hydromagnesite Mineral. *Thermochim. Acta* **2017**, *647*, 70−80.
(49) Zhang, C.; Shi, M.; Zhang, Y.; Yang, W.; Jiao, Z.; Yang, L. EG/TPU Composites with Enhanced Flame Retardancy and Mechanical Properties Prepared by Microlayer Coextrusion Technology. *RSC Adv.* **2019**, *9*, 23944−23956.
(50) Luo, Y.; Xie, Y.; Geng, W.; Dai, G.; Sheng, X.; Xie, D.; Wu, H.; Mei, Y. Fabrication of Thermoplastic Polyurethane with Functionalized MXene towards High Mechanical Strength, Flame-Retardant, and Smoke Suppression Properties. *J. Colloid. Interface Sci.* **2022**, *606*, 223−235.
(51) Afshari, M.; Dinari, M. A Novel Triazine-Based Covalent Organic Framework: Enhancement Fire Resistance and Mechanical Performances of Thermoplastic Polyurethanes. *Compos. A Appl. Sci. Manuf.* **2021**, *147*, No. 106453.
(52) Li, L.; Jiang, K.; Qian, Y.; Han, H.; Qiao, P.; Zhang, H. Effect of Organically Intercalation Modified Layered Double Hydroxides-Graphene Oxide Hybrids on Flame Retardancy of Thermoplastic Polyurethane Nanocomposites. *J. Therm. Anal. Calorim.* **2020**, *142*, 723−733.
(53) Zhou, K.; Gong, K.; Zhou, Q.; Zhao, S.; Guo, H.; Qian, X. Estimating the Feasibility of Using Industrial Solid Wastes as Raw Material for Polyurethane Composites with Low Fire Hazards. *J. Cleaner Prod.* **2020**, *257*, No. 120606.
(54) Huang, W.; Huang, J.; Yu, B.; Meng, Y.; Cao, X.; Zhang, Q.; Wu, W.; Shi, D.; Jiang, T.; Li, R. Facile Preparation of Phosphorus Containing Hyperbranched Polysiloxane Grafted Graphene Oxide Hybrid Toward Simultaneously Enhanced Flame Retardancy and Smoke Suppression of Thermoplastic Polyurethane Nanocomposites. *Compos. A Appl. Sci. Manuf.* **2021**, *150*, No. 106614.
(55) Liu, L.; Zhu, M.; Shi, Y.; Xu, X.; Ma, Z.; Yu, B.; Fu, S.; Huang, G.; Wang, H.; Song, P. Functionalizing MXene towards Highly Stretchable, Ultratough, Fatigue and Fire-Resistant Polymer Nanocomposites. *Chem. Eng. J.* **2021**, *424*, No. 130338.
(56) Lu, J.; Jia, P.; Liao, C.; Xu, Z.; Chu, F.; Zhou, M.; Yu, B.; Wang, B.; Song, L. Leaf Vein-Inspired Engineering of MXene@SrSn(OH)6 Nanorods towards Super-Tough Elastomer Nanocomposites with Outstanding Fire Safety. *Compos. B Eng.* **2022**, *228*, No. 109425.
(57) He, L.; Shi, Y.; Wang, Q.; Chen, D.; Shen, J.; Guo, S. Strategy for Constructing Electromagnetic Interference Shielding and Flame Retarding Synergistic Network in Poly (Butylene Succinate) and Thermoplastic Polyurethane Multilayered Composites. *Compos. Sci. Technol.* **2020**, *199*, No. 108324.
(58) Cai, W.; Wang, B.; Liu, L.; Zhou, X.; Chu, F.; Zhan, J.; Hu, Y.; Kan, Y.; Wang, X. An Operable Platform towards Functionalization of Chemically Inert Boron Nitride Nanosheets for Flame Retardancy and Toxic Gas Suppression of Thermoplastic Polyurethane. *Compos. B Eng.* **2019**, *178*, No. 107462.
(59) Wang, J.; Zhang, D.; Zhang, Y.; Cai, W.; Yao, C.; Hu, Y.; Hu, W. Construction of Multifunctional Boron Nitride Nanosheet towards Reducing Toxic Volatiles (CO and HCN) Generation and Fire Hazard of Thermoplastic Polyurethane. *J. Hazard. Mater.* **2019**, *362*, 482−494.
(60) Chen, H.; Deng, C.; Zhao, Z.; Wan, L.; Yang, A.; Wang, Y. Novel Piperazine-Containing Oligomer as Flame Retardant and Crystallization Induction Additive for Thermoplastics Polyurethane. *Chem. Eng. J.* **2020**, *400*, No. 125941.
(61) Chen, H.; Deng, C.; Zhao, Z.; Huang, S.; Wei, Y.; Wang, Y. Novel Alkynyl-Containing Phosphonate Ester Oligomer with High Charring Capability as Flame Retardant Additive for Thermoplastic Polyurethane. *Compos. B Eng.* **2020**, *199*, No. 108315.
(62) Yang, A.; Deng, C.; Chen, H.; Wei, Y.; Wang, Y. A Novel Schiff-Base Polyphosphate Ester: Highly-Efficient Flame Retardant for Polyurethane Elastomer. *Polym. Degrad. Stab.* **2017**, *144*, 70−82.
(63) Zhang, S.; Liu, X.; Jin, X.; Li, H.; Sun, J.; Gu, X. The Novel Application of Chitosan: Effects of Cross-Linked Chitosan on the Fire Performance of Thermoplastic Polyurethane. *Carbohyd. Polym.* **2018**, *189*, 313−321.
(64) Liu, L.; Xu, Y.; He, Y.; Xu, M.; Shi, Z.; Hu, H.; Yang, Z.; Li, B. An Effective Mono-Component Intumescent Flame Retardant for the Enhancement of Water Resistance and Fire Safety of Thermoplastic Polyurethane Composites. *Polym. Degrad. Stab.* **2019**, *167*, 146−156.
(65) Jiao, C.; Zhang, Y.; Dong, H.; Chen, W.; Liu, W.; Li, S.; Chen, X. Novel Phenolic Resin Hollow Microspheres: Flame Retardancy and Toxicity Reduction in Thermoplastic Polyurethane Elastomer. *Express Polym. Lett.* **2021**, *15*, 887−898.
(66) Zhang, Y.; Cui, J.; Wang, L.; Liu, H.; Yang, B.; Guo, J.; Mu, B.; Tian, L. Phosphorus-Containing Salen-Metal Complexes Investigated for Enhancing the Fire Safety of Thermoplastic Polyurethane (TPU). *Polym. Adv. Technol.* **2020**, *31*, 1150−1163.
(67) Cui, M.; Li, J.; Gao, Q.; Xiang, J.; Chen, Y.; Yan, J.; Fan, H. A Novel Strategy to Fabricate Nylon 6 Based Flame Retardant Microfiber Nonwoven Fabric with Durability. *Colloid Surf. A* **2022**, *641*, No. 128482.
(68) Tan, W.; Ren, Y.; Guo, Y.; Liu, Y.; Liu, X.; Qu, H. A Novel Multi-Claw Reactive Flame Retardant Derived from DOPO for Endowing Lyocell Fabric with High Effective Flame Retardancy. *Cellulose* **2022**, *29*, 6941−6962.
(69) Mu, X.; Zhan, J.; Feng, X.; Yuan, B.; Qiu, S.; Song, L.; Hu, Y. Novel Melamine/o-Phthalaldehyde Covalent Organic Frameworks Nanosheets: Enhancement Flame Retardant and Mechanical Performances of Thermoplastic Polyurethanes. *ACS Appl. Mater. Interfaces* **2017**, *9*, 23017−23026.
(70) Singh, K.; Mishra, A.; Kumar, N.; Tripathi, D.; Shami, T. Evaluation of Thermal, Morphological and Flame-Retardant Properties of Thermoplastic Polyurethane/Polyphosphazene Blends. *Polym. Bull.* **2017**, *75*, 2415−2430.
(71) Ning, N.; Yan, B.; Liu, S.; Yao, Y.; Zhang, L.; Chan, T.; Nishi, T.; Tian, M. Improved Actuated Strain of Dielectric Elastomer Through Disruption of Hydrogen Bonds of Thermoplastic Polyurethane by Adding Diaminonaphthalene. *Smart Mater. Struct.* **2015**, *24*, No. 032002.
(72) Schartel, B.; Hull, T. Development of Fire-Retarded Materials-Interpretation of Cone Calorimeter Data. *Fire Mater.* **2007**, *31*, 327−354.
(73) Wei, Y.; Zhu, S.; Qian, Q.; Jiang, Q.; Zhang, L.; Jin, K.; Liu, W.; Qiu, Y. Hexachlorocyclotriphosphazene Functionalized Lignin as a Sustainable and Effective Flame Retardant for Epoxy Resins. *Ind. Crop. Prod.* **2022**, *187*, No. 115543.
(74) Li, D.; Liu, L.; Zhang, Z.; Xu, M.; Xu, Y.; Qian, L. An Urethane-Based Phosphonate Ester for Improving Flame Retardancy and Smoke Suppression of Thermoplastic Polyurethane. *Polym. Degrad. Stab.* **2021**, *188*, No. 109568.
(75) Chen, L.; Zeng, S.; Xu, Y.; Nie, W.; Zhou, Y.; Chen, P. Epoxy-Modified Silicone Resin Based N/P/Si Synergistic Flame-Retardant Coating for Wood Surface. *Prog. Org. Coat.* **2022**, *170*, No. 106953.

https://doi.org/10.1021/acsomega.3c01464
ACS Omega 2023, 8, 18151−18164

(76) Yin, Z.; Cai, W.; Lu, J.; Yu, B.; Wang, B.; Song, L.; Hu, Y. Cost-Effective Graphite Felt and Phosphorous Flame Retardant with Extremely High Electromagnetic Shielding. *Compos. B Eng.* **2022**, *236*, No. 109819.
(77) Liu, C.; Yang, D.; Sun, M.; Deng, G.; Jing, B.; Wang, K.; Shi, Y.; Fu, L.; Feng, Y.; Lv, Y.; Liu, M. Phosphorous-Nitrogen Flame Retardants Engineering MXene towards Highly Fire Safe Thermoplastic Polyurethane. *Compos. Commun.* **2022**, *29*, No. 101055.
(78) Wang, Y.; Liu, L.; Ma, L.; Yuan, J.; Wang, L.; Wang, H.; Xiao, F.; Zhu, Z. Transparent, Flame Retardant, Mechanically Strengthened and Low Dielectric EP Composites Enabled by a Reactive Bio-Based P/N Flame Retardant. *Polym. Degrad. Stab.* **2022**, *204*, No. 110106.
(79) Wang, Y.; Ma, L.; Yuan, J.; Zhu, Z.; Liu, X.; Li, D.; He, L.; Xiao, F. Furfural-Based P/N/S Flame Retardant Towards High-Performance Epoxy Resins with Flame Retardancy, Toughness, Low Dielectric Properties and UV Resistance. *Polym. Degrad. Stab.* **2023**, *212*, No. 110343.

https://doi.org/10.1021/acsomega.3c01464
ACS Omega 2023, 8, 18151−18164